

RECENT APPLICATIONS OF CFD MODELING IN THE POWER GENERATION, METALS AND PROCESS INDUSTRIES

Philip J STOPFORD

AEA Technology Engineering Software, Harwell, Oxfordshire OX11 0RA, UK

ABSTRACT

Computational Fluid Dynamics (CFD) modeling is now widely applied as an industrial plant development and process optimization tool. The steady increase in computer power over recent years has enabled process engineers to model reacting multi-phase flows in a realistic geometry with good mesh resolution. As a result, the number of applications of CFD to industrial processes is also growing rapidly and increasing in sophistication.

This paper reviews some of the recent applications of the CFX-4 code of AEA Technology (1997) to the Power Generation, Process and Metals Industries. The aim is to illustrate what can be done and also to identify trends and those areas where further work is needed. Examples include coal-fired low-NO_x burner design, furnace optimization, over-fire air, gas reburn, laminar flames, reformers, chemical reactors and continuous metal casting. It is argued that the trend is for CFD models to become more comprehensive and accessible by being coupled to other process models and embedded in automated information and process control systems.

INTRODUCTION

Many industrial processes involve multi-phase flow, phase transformation and complex chemical reactions linked with conjugate heat transfer. This is particularly true of the power generation and the minerals and metals processing industries; examples include pulverized coal combustion, ore sintering, metal casting, mould filling and mixing vessel. Although standard CFD models of single-phase turbulent flow and heat transfer can provide a qualitative understanding of some of these processes, well-validated multi-phase models are needed before CFD can be used with confidence as an engineering design tool.

COAL FURNACE SIMULATION

Low NO_x Burner Design

International Combustion Limited (now ABB Combustion Systems) have developed a family of modern low-NO_x burners which incorporate both air and fuel staging. To optimize the performance of the burner in specific applications, CFX-4 has been used to calculate isothermal and combusting flows, in both single burner and multi-burner furnace simulations.

The burner, shown in Figure 1, has three concentric inlets: nearest the axis is the pulverized fuel and primary air pipe with collectors and wedges to promote angular bunching and radial spreading of the coal, then highly-swirled

secondary air register, and; finally unswirled tertiary air with blockers at the exit. The essential internal features are reproduced in the CFD model of a 90° sector shown in Figure 2. Secondary air swirl was simulated in the model by momentum sources.

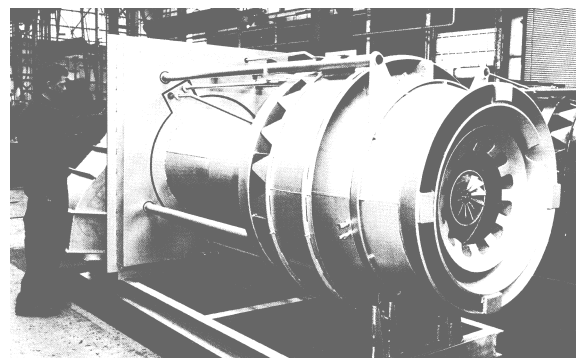
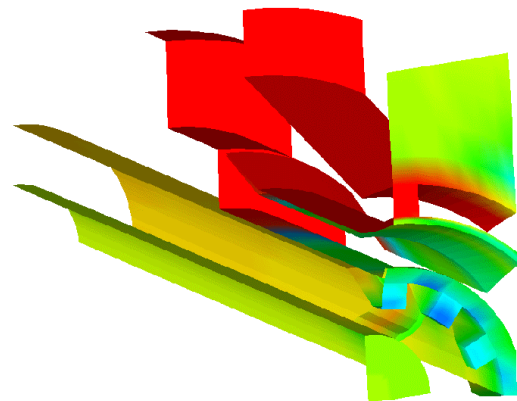


Figure 1: ABB Combustion Systems Low-NO_x burner.



CFX

Figure 2: CFX-4 90° sector model of low NO_x burner.

To validate the CFD model, predictions were compared with extensive LDA data for isothermal flow in a 1/2-scale burner model. To simulate the presence of the laboratory floor and walls during the measurements, the burner flow was modeled in a box of 4.67m width and 6m long.

Results were obtained for meshes of 28,000 and 82,000 cells, the standard and RNG k- ϵ turbulence models and with hybrid and CONDIF upwind differencing schemes. Typical radial profiles of axial velocity can be seen in Figures 3 and 4. Good agreement for the axial and swirl velocities was obtained with the measurements for most

cases although the fine mesh and the CONDIF scheme performing best.

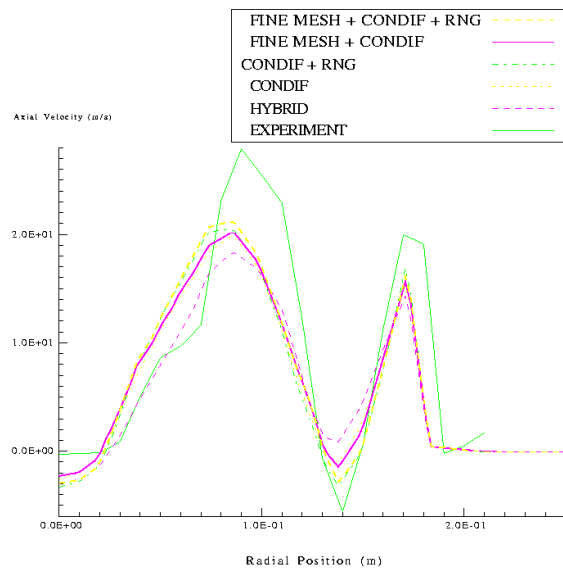


Figure 3: Comparison of CFX-4 with LDA velocity data at the burner exit of 1/2-scale isothermal model.

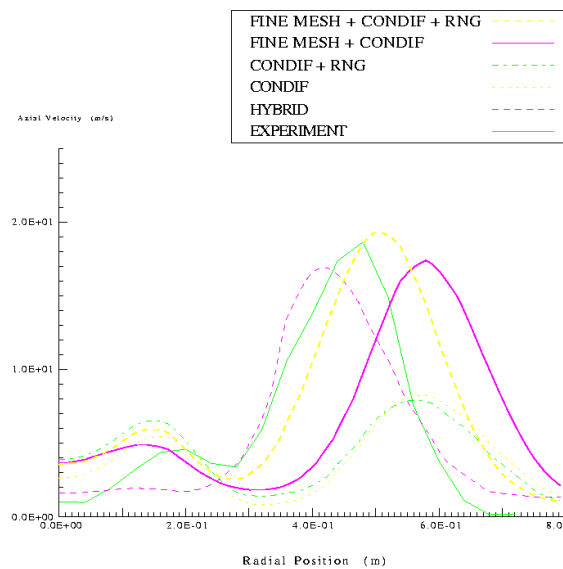


Figure 4: Comparison of CFX-4 with measurements 0.8m downstream of the burner exit.

The burner model was subsequently incorporated into multi-burner furnace models as part of the "ACORDE" project supported by the European Commission. One of these calculations was for a unit of the Sines Power Station operated by Electricidade de Portugal (EDP). The EDP Sines Plant has four similar units, each of 314 MW_e nominal capacity and began operation in 1985. Units 1 and 2 have recently been retrofitted with low-NOx burners and an over-fire air system mounted on the front wall. The plant burns blends of pulverized bituminous coal using the direct firing dry bottom method and each unit has 20 burners mounted in five rows on the front-wall. The units are of conventional design except that a small amount of boundary air is admitted through slots between tubes at

the hopper throat to combat reducing conditions on the furnace walls.

The furnace model included superheater platens and exploited the center-line symmetry to model only half the furnace. Furnace calculations were performed on a mesh of 360,000 cells and 5,000 representative coal particles were simulated. Results for full-load baseline cases with and without over-fire and with a change to the firing pattern air show reasonably good agreement with measured NOx data (within about 10%) but less good agreement for carbon-in-ash (see Table 1). This is thought to be due to the neglect of char oxidation by CO₂ and H₂O. Plots of temperature and NO concentration for the 15% over-fire air case are shown in Figures 5 and 6. The vertical X-Y plane in these figures is the center-line symmetry plane.

Results	Over-fire Air %	Firing Pattern	Predicted	Measured
NOx ppm @6% O ₂	0	1-5	476	500
	15	1-5	264	297
	20	2-5	300	320
Carbon-in-Ash %	0	1-5	7.3	4.0
	15	1-5	6.7	3.8
	20	2-5	12.7	5.7

Table 1: Comparison of CFX NOx emission and char burn-out predictions with the measurements at the Sines Power Plant.

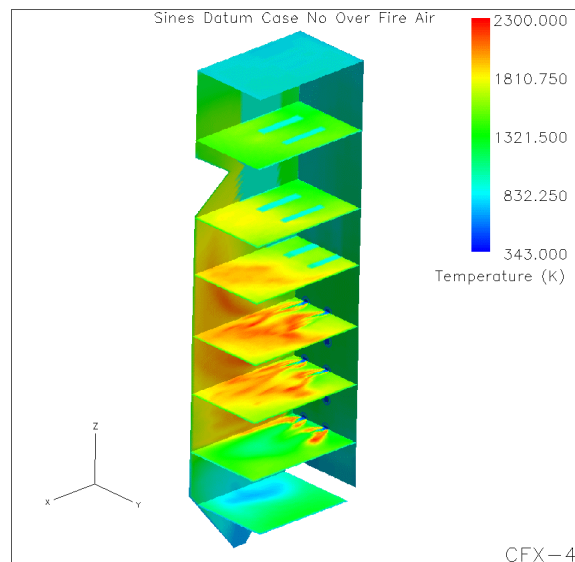


Figure 5: CFX predictions for in-furnace temperature for the Sines furnace.

Effects of Coal Quality

AEA Technology is one of the sub-contractors in the project "The Effect of Coal Quality on NOx Emissions and Carbon Burn-Out in Pulverized Coal Utility Boilers"

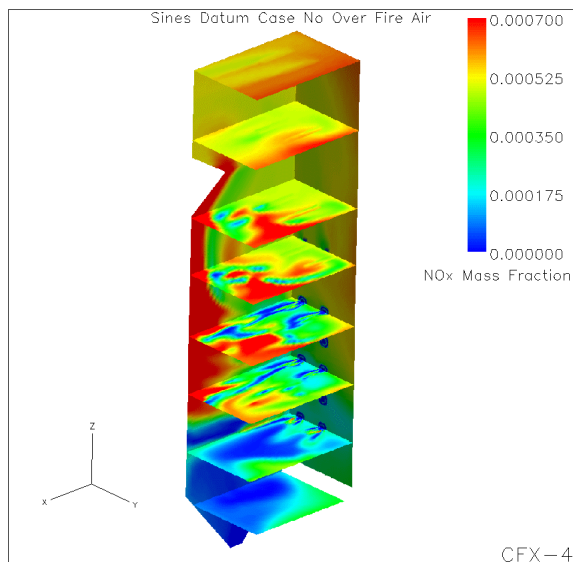


Figure 6: CFX predictions for NO mass fraction for the Sines furnace.

coordinated by National Power and partially sponsored by the UK Department of Trade and Industry. The project has three elements: laboratory-scale coal characterization; large-scale testing on single-burner rigs and full-scale power plant and mathematical modeling, including heat balance modeling and computational fluid dynamics (CFD) simulation of in-furnace combusting flow and NOx formation and destruction. The main aim is to predict NOx and Loss of Ignition (or char burn-out) to within 5% for a suite of eight coals fired in furnaces at three different scales (160 kW, 40 MW and full-scale). For a summary of the whole project, see O'Connor (1999).

Having demonstrated good agreement between single-burner models and the measurements, the main task of the project was to predict the behavior of the test coals when fired on full-scale multi-burner furnaces. The 7 trials to be simulated were on two nominally-identical 500MWe front wall-fired furnaces at Didcot and Ratcliffe (operated by National Power and PowerGen respectively) with 48 Mitsui-Babcock low NOx burners (4 rows of 12). Table 2 summarizes the conditions of each trial; note that the furnaces can operate at full load even with two mills out of service.

Trial	Coal	Mills Out of Service	Excess O ₂ (%) ¹
1	Pittsburgh #8	DE	7.5
2	"	"	6.5
3	"	"	7.0
4	Asfordby	AG	6.08
5	"	"	5.48
6	Betts Lane	BG	6.1
7	"	"	5.85

Table 2: Conditions for power station trials.

¹The 312,000-cell furnace model included the platens in detail to ensure that char particle time-temperature histories were correctly modeled and had extra refinement

¹ At air heater inlet.

in the region of the burner belt. The size of the model was reduced by exploiting the symmetry about the vertical furnace center-line. Furnace air in-leakage, so-called "tramp" air, of approximately 15% of the total furnace air, had to be included explicitly to obtain reasonable NOx and char burn-out predictions. Details of the mesh and typical results are shown in Figures 7, 8 and 9.

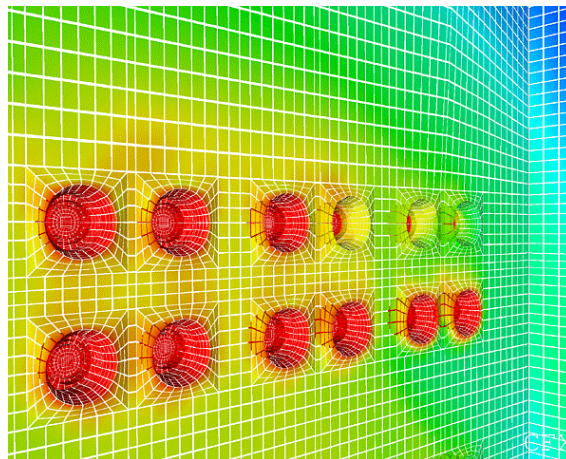


Figure 7: Close-up of mesh around wall-fired burners in the Didcot/Ratcliffe furnace model.

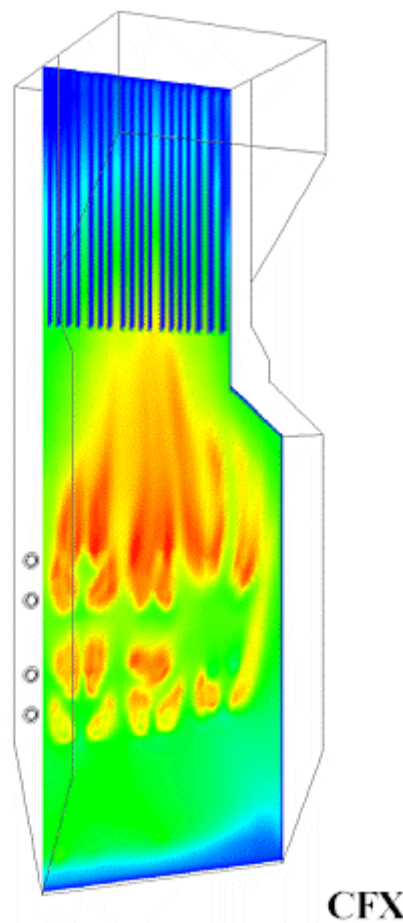


Figure 8: Predicted temperature in the mid-plane for the Trial 1#2 calculation.

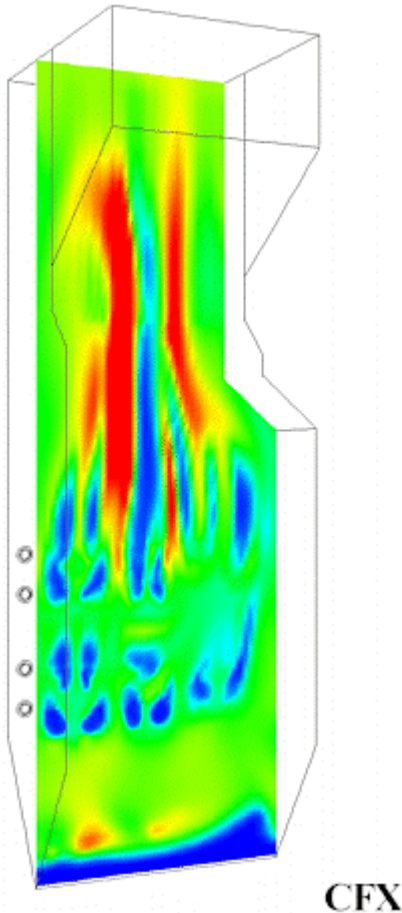


Figure 9: Predicted NO_x in the mid-plane for the Trial 1#2.

The predictions and measured values for NO_x and Gross Calorific Value (GCV) loss for the power-station furnace simulations are shown in Table 3. The predicted NO_x levels are within 15% of the measured values and show the correct trend with variation of excess O₂. Given accurate air flow boundary conditions at high oxygen levels (e.g. the Asfordby datum case, Trial 4), CFX-4 can predict exit plane NO_x values to within 5% of the measured value.

It is important that, in addition to burner flow rates, leakage air is accurately specified. This is shown by the Pittsburgh #8 datum calculation, Trial 1#1, where NO_x levels were over-predicted. It is believed that leakage flows were larger in the Didcot furnace, leading to an overestimate in the calculations of the oxygen level near the burners producing the over-prediction of exit plane NO_x. The reduction in NO_x in going from Pittsburgh to Asfordby coals is correctly predicted but the prediction for Betts Lane is below the measured value, suggesting that the level of oxygen in the furnace was underestimated when setting the model boundary conditions.

Trends are also correctly predicted for GCV loss although the absolute value was over-predicted, indicating that the reaction of char with species other than oxygen, probably H₂O or CO in the product gas, is making a small but still

Calculation	Leakage air removed	Coal Bias	Air Bias	GCV Loss (%)	NO _x ¹ (ppm)
Trial 1#1	no	no	no	0.17	419
#2	yes	no	no	2.07	346
#3	yes	yes	no	2.17	349
#4	yes	yes	yes	2.41	347
Measured				1.65	306
Trial 2	yes	no	no	6.01	277
Measured				3.47	240
Trial 3	yes	no	no	3.11	313
Measured				2.54	260
Trial 4#1	yes	no	no	1.95	300
#2	yes	yes	no	1.88	290
#3	yes	yes	yes	1.84	300
Measured				0.71	299
Trial 5	yes	yes	yes	3.12	271
Measured				0.83	253
Trial 6#1	yes	no	no	4.88	232
#2	yes ²	no	no	2.21	278
Measured				3.04	330
Trial 7	yes	no	no	5.42	216
Measured				3.01	305

Table 3: CFX-4 results for UK power station boilers.¹

significant contribution to char burn-out. This mechanism should be more important at lower oxygen levels and is reflected in the less accurate predictions of both GCV loss and exit plane NO_x for the low oxygen tests. Comparison between the three coals, Asfordby, Pittsburgh #8 and Betts Lane, shows that the correct trend is predicted for unburned carbon loss with the loss increasing from Asfordby to Pittsburgh to Betts Lane (i.e. GCV loss increased as volatile matter decreased).

Application of both biased coal and air distributions had only a small effect on predictions but flow distributions were strongly affected by the configuration of active mills. This makes comparison of predictions for different coal types difficult, since different mill configurations were used for the Pittsburgh #8, Asfordby and Betts Lane tests. Both Asfordby and Pittsburgh #8 coals produce similar measured exit plane NO_x levels and this is reflected in the calculations when allowance is made for the different leakage rates at Ratcliffe and Didcot. The high measured NO_x levels for the Betts Lane coal appear anomalous, since furnace oxygen levels were below the values in both the Asfordby and Pittsburgh #8 tests. The increasing value of GCV loss when changing from Asfordby to Pittsburgh #8 to Betts Lane coals was correctly as were the trends in both exit plane NO_x and GCV loss with changes in oxidant levels.

The conclusions of this work are:

- Correct trends in NO_x and GCV loss (char burn-out) can be achieved for multi-burner furnace calculations providing that the inlet boundary conditions, burner inlet profiles and furnace air in-leakage are set correctly.

¹ At 6% O₂.

² For this calculation an extra 7% combustion air was added to give the same air leakage through the air heater as the Trial 4.

- Absolute values for NO_x are within 15% of the measured values and, when the furnace conditions are accurately known, within 10%. GCV loss is difficult to predict within 30% because a small error in the char burn-out prediction gives a large error in the GCV loss.
- Under-prediction of GCV loss in all cases suggests improvements in the char oxidation model to include char reactions with combustion products are needed.

Over-Fire Air in Cyclone Boiler

The aim of this study was to evaluate the NO_x reduction achieved by various designs of over-fire air installation in a Babcock and Wilcox cyclone boiler. Cyclone boilers fuelled by crushed coal differ from the more conventional corner and wall-fired units burning pulverized coal in that coal pyrolysis and char oxidation takes place in a separate high-temperature chamber, the cyclone furnace, attached to each burner prior to the hot gaseous products entering the main boiler furnace where most of the heat is extracted.

The purpose of the cyclone furnace is to retain most of the coal ash for subsequent tapping off as semi-molten slag. To achieve this, the residence time of the crushed coal particles in the cyclone furnace is increased by generating a high-swirled flow region and ash deposition is promoted by attaching refractory to the tube walls to increase the surface temperature and, hence, the capacity of the ash to stick to the wall. See Figures 10 and 11.

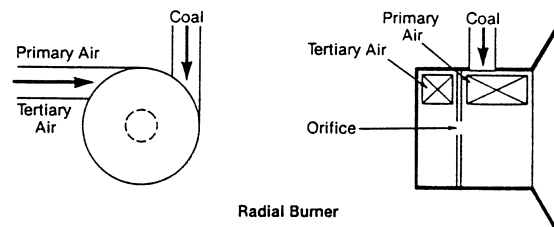


Figure 10: Schematic of a radial cyclone furnace.

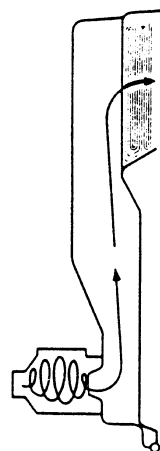


Figure 11: Schematic of a cyclone boiler showing a typical coal particle trajectory.

The standard CFX-4 coal combustion model was used for the cyclone furnace calculations but with a modification to the behavior of the Lagrangian particles near walls. Particles were captured and their char fully burned-out on wall impact if either the wall or local gas temperature were above the “T250” slagging temperature for the coal being modeled. If the particles were not captured they were assumed to rebound from the wall with a coefficient of restitution of 0.5.

The starting location for the coal particles was set at random where the coal hopper enters the cyclone burner, with a random velocity ranging between 0.17 and 3.8 m/s; the minimum velocity corresponds to an assumed volume fraction of 50% in the coal feeder, with the coal passing through a hole of diameter 9.75 inches and the maximum velocity corresponds to a coal particle free-falling through a distance of 30 inches.

Six different over-fire air arrangements were evaluated as well as a datum case without over-fire air for comparison. The results are summarized in Table 4.

Case No.	1	2	3	4	5	6	7
Cyclone Stoich.	1.09	0.95	1.0	0.95	0.95	1.0	1.0
Over-fire Air (%)	0	14.2	9.6	11.3	14.2	9.6	7.7
Biased OFA	-	No	Yes	Yes	Yes	Yes	Yes
OFA Port Height	-	High	High	High	Low	Low	Low
Under-fire Air (%)	0	0	0	2.9	0	0	1.9
Top Of Nose:							
O ₂ Dry (vol. %)	2.08	2.42	2.20	2.15	2.14	2.22	2.17
Temperature (°C)	1189	1180	1181	1189	1194	1186	1186
NO _x Dry at 3% O ₂ (ppm vol)	574	208	279	234	186	278	302
CO Dry at 3% O ₂ (ppm vol)	11.1	7.2	5.2	6.2	6.0	5.0	6.3
Exit Plane:							
O ₂ Dry (vol. %)	2.06	2.14	2.10	2.03	2.02	2.08	2.08
Temperature (°C)	1029	1021	1025	1028	1031	1029	1032
NO _x Dry at 3% O ₂	572	209	280	237	188	282	302
CO Dry at 3% O ₂	0.3	0.2	0.2	0.3	0.2	0.2	0.2
Char Burn-out (%)	99.3	98.5	98.8	99.5	99.7	99.2	98.9
Carbon In Ash (%)	3.2	6.4	5.3	2.4	1.2	3.8	4.8

Table 4: Summary of CFX-4 predictions for cyclone furnace with various NO_x reduction strategies.

The calculations indicate that the level of unreacted char is not greatly affected by the introduction of over-fire air. This is due to the design of the cyclone furnace where the majority of particles react on the cyclone and furnace walls. Part of this insensitivity of unburned char to changes in cyclone stoichiometry might be due to the modeling assumption that any coal particle that sticks on a cyclone wall burns out fully.

The results showed that substantial reductions in NO_x (over 50%) could be achieved by using 9.6 to 14.2% over-fire air on the rear wall. The calculations also indicate that switching air from the over-fire air ports, to under-fire air ports below the cyclones results in an increase in both the

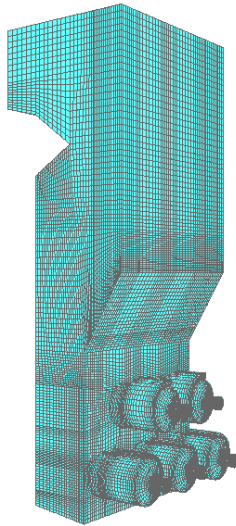


Figure 12: Finite-volume mesh of about 300,000 cells for a boiler with five cyclone furnaces.

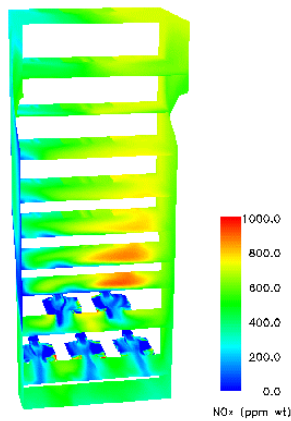


Figure 13: NO mass fraction for the baseline cyclone boiler Case 1 with no over-fire air.

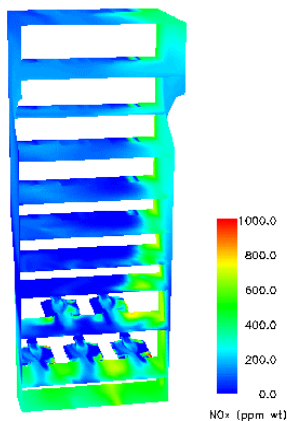


Figure 14: NO for the optimum low NOx configuration of cyclone boiler (Case 5) with 14.2% over-fire air and no under-fire air.

NO_x produced and the unburned char. Furthermore, it has been demonstrated that the introduction of a biased over-

fire air flow improves the air distribution and, in particular, reduces the size of a low oxygen region near the southern side wall of the furnace above the cyclones. This work shows how CFD can be used to bias air flow rates in over-fire air systems in order to maximize their effectiveness in reducing NO_x.

NO_x Reburn in Corner-Fired Furnaces

Fuel-lean gas reburn (FLGR) involves injection of natural gas into furnace flue gas in order to create reducing conditions local to the gas jets and so reduce some of the NO_x. The Gas Research Institute in association with US utilities has demonstrated a NO_x reduction of 30-45% with a gas consumption of 5-7% of the boiler heat input. Since FLGR does not need the over-fire air system of a conventional reburn system the cost of installation per kW is only about US\$8 compared with US\$35 for the conventional system.

CFX-4 has been used to assess the potential NO_x reduction from FLGR in a 350 MWe corner-fired furnace. The furnace has four tilttable windbox assemblies located at the corners of the furnace. Each windbox assembly is divided into 11 compartments: the five PF nozzles alternating with secondary air inlets, each consisting of a straight nozzle with a horizontally-offset nozzle above and below. In addition, separate over-fire air is introduced through two levels of corner-mounted upward-tilting nozzles just above the burner boxes. Natural gas was introduced through 11 sonic nozzles just below the furnace nose at locations that were optimized by CFD calculation to give the best NO_x reduction. The reburn process was represented in the model by the single global reaction model of Chen et al. (1996) ($\text{NO} + \text{CH}_i \rightarrow \text{HCN} + \dots$) with the reaction rate $2.72 \times 10^6 e^{-18,800/RT}$ gmol/cm³s.

As well as the reduction in fuel NO resulting from the decrease in the coal input to the upper coal level (to compensate for the thermal input of the gas), there is a significant amount of reburn that can reduce NO_x by as much as 50%. The predicted NO_x is compared with the current and proposed US limits in Table 5.

	ppm (Vol. dry @ 6% O ₂)	lb./mBTU
Without FLGR	260	0.43
With 5% FLGR	128	0.21
Current US limit	270	0.45
Proposed US limit	90	0.15

Table 5: CFD predictions of NO_x emissions with and without optimum level of FLGR and corresponding current and proposed US limits for coal-fired plant.

In practice it is difficult to realize all of the predicted reduction because of the practical difficulty of operating at low air-to-fuel ratios. However, the lean gas reburn technique has been demonstrated to give 30% NO_x reductions at very low cost (a factor of 5 lower than a conventional gas reburn system) when CFD is used to target the gas injection to form sub-stoichiometric regions in corner-fired furnaces. Although the reductions are substantial and worthwhile they may still be insufficient to meet the proposed statutory limit without the use of other NO_x reduction techniques.

0.00050
0.00045
0.00040
0.00035
0.00030
0.00025
0.00020
0.00015
0.00010
0.00005
0.00000

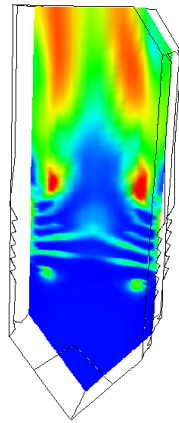


Figure 15: NO mass fraction for corner-fired furnace without FLGR.

0.00020
0.00016
0.00012
0.00008
0.00004
0.00000
-0.00004
-0.00008
-0.00012
-0.00016
-0.00020

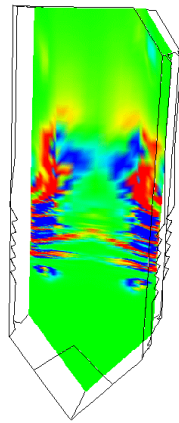


Figure 16: NO production rate (in kg/m³/s) without FLGR.

0.00050
0.00045
0.00040
0.00035
0.00030
0.00025
0.00020
0.00015
0.00010
0.00005
0.00000

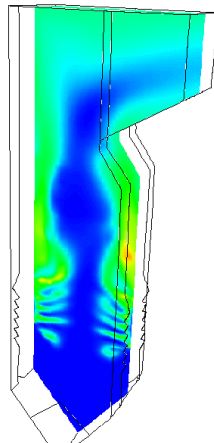


Figure 17: NO mass fraction for corner-fired furnace with 5% gas injection FLGR below furnace nose.

0.00020
0.00016
0.00012
0.00008
0.00004
0.00000
-0.00004
-0.00008
-0.00012
-0.00016
-0.00020

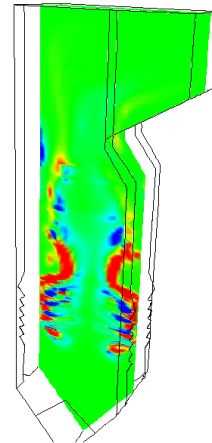


Figure 18: NO production rate (in kg/m³/s) with FLGR.

Overall Conclusions of Coal Combustion Modeling

- CFD modeling is now well established as a design tool for burner and furnace design. It has been widely applied in the power generation industry to help combustion engineers reduce emissions, increase thermal efficiency, select fuels and extend plant lifetime;
- CFD models are capable of predicting furnace NO_x emissions within 10% provided that the operating conditions of the boiler are well-characterized. The method has been successfully applied to wall-fired, corner-fired and cyclone furnaces using the same sub-models and parameters in all cases;
- Char burn-out is more difficult to predict accurately but trends are usually indicated correctly which is often all that is required for design purposes. Further basic research is needed to characterize char oxidation rates at high-levels of burn-out;
- With careful application to well-characterized plant conditions, CFX-4 is a powerful tool for the analysis of combusting flow in a coal-fired multi-burner power station furnace.

COUPLED CHEMICAL KINETICS

The standard solution method in CFX-4 for the flow, is based upon a segregated solution algorithm, where the momentum equations are solved one by one, and the pressure is updated from the equation of mass conservation. For reacting flow problems, there are additional equations for the concentration or mass fraction of each species, and their interactions. For single-phase non-buoyant flows, the only feedback between the chemistry and the flow arises through the density variation caused by exothermic or endothermic reactions. For example, in combustion, the heat of reaction increases the temperature and reduces the density.

In the methods adopted here, the equations for the mass fractions are split into two parts, transport (advection and diffusion) and reaction. Schematically, the transient non-linear equations for each of the mass fractions can be written as

$$\partial\phi / \partial t + F(\phi) - C(\phi) = 0 \quad (1)$$

where ϕ is the conserved quantity. In this equation the operator F represents the flow part of the equation, for the advection and diffusion of the species, and C represents the chemical interactions between the species.

Note that operator C is entirely local, and only involves values at center of each control volume, whereas the operator F is non-local and involves the transport of the species from neighboring points.

These equations are discretized in the usual manner for CFX-4, using a finite volume approach. The operator F can be further split into a component arising from the center of the control volume F_D and a contribution from neighboring control volumes, through convection and diffusion, F_N , so that

$$F = F_D + F_N$$

The fractional step method adopted here for advancing the solution from time level n to $n+1$ can be written as:

Step One, Implicit Chemistry Step

$$\partial\phi^*/\partial t - C(\phi^*) + F_D(\phi^*) = -F_N(\phi^n) \quad (2)$$

Step Two, Implicit Flow Step

$$\partial\phi^{n+1}/\partial t + F_N(\phi^{n+1}) + F_D(\phi^{n+1}) = C(\phi^*) \quad (3)$$

The values ϕ^* can be considered as values at some intermediate time level between n and $n+1$. The left-hand side of equation (2) contains only chemical and thermodynamic source terms, together with the 'diagonal' contribution from the flow term. These are all local to each computational cell.

The time derivatives in these equations are discretized using the standard CFX time discretizations, for example, first or second order backward difference formulae. With a first order backward difference, for example,

$$\partial\phi/\partial t|_{n+1} = (\phi^{n+1} - \phi^n) / (t^{n+1} - t^n) \quad (4)$$

For steady state problems, the time steps are false time steps, chosen to accelerate convergence to a steady state, with different values adopted for each of the flow and chemistry time steps. This approach has the advantage that physical arguments can be applied to obtain suitable values for the false time steps. This is discussed in more detail later.

Linearization of the Chemical Equations

The equations for the chemical species (2) are coupled and highly non-linear and need to be linearized. The effect of temperature is highly non-linear, through the equation of state and the Arrhenius reaction rates, and it is important to include this in the linearization. The 'chemistry' equation set is therefore extended to include the transport equation for the enthalpy and the enthalpy-temperature relationship, which is a purely algebraic relationship. The variables chosen for the linearization, and subsequent solution, are the mass fractions of the chemical species, the enthalpy and the temperature, so that the scalars in each control volume can be written in vector form as

$$\phi = \begin{matrix} Y_i, & i = 1 \text{ to } N \\ H, \\ T, \end{matrix}$$

where the Y_i are the mass fractions of the chemical species, N is the number of chemical species, H is the enthalpy and T is the temperature.

The chemical equations are specified to CFX-4 either interactively, or through the CFX Command Language. This high level input allows a flexible specification of the chemical equations, and the reaction rates.

As the structure of the equations is known, the Newton linearization is carried out automatically for the chemical interactions, using analytic differentiation, and the chain rule. This enables the Jacobian of the chemical equations to be determined cheaply. For non-Arrhenius rate expressions, the additional components of the Jacobian have to be specified analytically.

Solution Schemes

In order to advance the solution through one time step, the following equations are solved:

1. The momentum and global mass conservation equations;
2. Reaction equations for the chemical species, the enthalpy and temperature equation, (2);
3. Convection - diffusion equation for the scalars, the chemical species and the enthalpy equation, (3).

Conventional segregated solution methods are used to solve the momentum and mass conservation equations for the flow step. For example, SIMPLEC is the default for the pressure-velocity coupling, the pre-conditioned conjugate gradient method for the pressure-correction equation and Stone's method or line relaxation for the linearized convection-diffusion equations for momentum, enthalpy and mass-fractions. These are iterated to meet the standard convergence criteria at each step, before carrying out the reaction correction.

The chemistry has now been reduced to the solution of a set of coupled non-linear equations for the vector ϕ^* representing the variables at each point,

$$(\phi^* - \phi^n) / (t^* - t^n) - C(\phi^*) = -F(\phi) \quad (5)$$

Adopting the Newton linearization, this results in a linear set of equations,

$$(\mathbf{I} - h \mathbf{J}) \phi^* = -h \mathbf{F}(\phi^n) + \phi^n \quad (6)$$

where \mathbf{I} is the identity matrix, \mathbf{J} is the Jacobian matrix, $\partial C/\partial \phi$, and h is the effective time step for the chemistry step.

For stability reasons, this equation is iterated to convergence. Note that the Jacobian matrix can be a singular matrix, and it is necessary to use a false transient approach for steady state solutions, in order to have a non-singular matrix. Gaussian elimination with partial pivoting is used to solve the linear equations.

Automatic Time Stepping

In order for the above numerical scheme to work well, it is essential to have an automatic time-stepping scheme, with the false time step increasing as a steady state is approached. Two false time steps are introduced for each control volume, one for the chemistry step, and one for the flow step. These time steps can be adjusted on the basis of the local behavior of the solution, so that convergence can be accelerated. The criteria adopted for adjusting these time steps are:

- A sufficiently small time chemistry false time step is set, to ensure that the iteration matrix ($\mathbf{I}-h\mathbf{J}$) remains non-singular, especially for strongly exothermic reactions, and converges well;
- Changes in the variables for each iteration are bounded;
- Mass fractions are not allowed to go negative, preventing unphysical intermediate results;
- For the flow step, the time scales are based upon the convection and diffusion time scales, rather than the chemical time scales.

A number of different variations of the algorithm have been tried, for example with different splittings of the equations, and different heuristics for the control of the false time steps. The algorithm has also evolved in the light of the practical experience gained on stiff systems of equations. The method described provides the best compromise for efficiency and robustness, although other variations are available within the software.

Laminar Flame Examples

The coupled chemistry solver has been applied, in collaboration with Gastec and the Technical University of Eindhoven, to simulate laminar combustion in the latest generation of compact domestic gas burners. Typically, these burners use a porous sintered metal element to stabilize the combustion of pre-mixed methane and air. Since the fuel is pre-mixed and the flow is laminar, the combustion rate is controlled by the chemical kinetics, rather than by the turbulent mixing processes, as with turbulent diffusion flames with fast chemistry.

The CFX model includes both the combusting flow downstream of the element and the non-combusting flow of reactants upstream and through the element. For completeness, the influence of a heat exchanger downstream of the burner surface is also included, which necessitates both conjugate heat transfer (i.e. conduction through solids) and radiation to be modelled. Radiative heat transfer from the flame to the surface of the porous element is thought to be an important stabilization mechanism in this type of burner. Since molecular diffusion determines the laminar flame thickness, fine mesh (about 10 cells per mm) was needed near the flame front and the calculation included temperature-dependent binary diffusion coefficients.

As a validation exercise, a 2-D bunsen burner flame was modeled by CFX using a single-step global methane-air reaction model developed at the Technical University of Eindhoven with the fuel consumption rate:

$$r = -A\rho^{\alpha+\beta}Y_f^\alpha Y_a^\beta e^{-T_a/T}$$

where $A = 2.6 \times 10^{15} (\text{kgm}^{-3})^{-3} \text{s}^{-1}$, $\alpha = 2.8$, $\beta = 1.2$ and $T_a = 16,900\text{K}$. Detailed comparisons were made between the CFX model and the LAMFLA2D software from Eindhoven University (Mallens, 1996). Figure 19 shows that the agreement between the two codes for the same reaction scheme is very good. The figures also shows the CFX results for the four-step scheme of Jones and Lindstedt (1988).

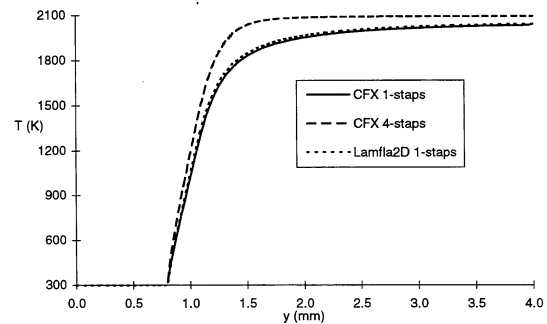


Figure 19: Temperature predictions for a 2-D flame showing comparison between CFX-4 and the Lamfla2D software for a one-step reaction scheme and the CFX-4 results for the four-step scheme.

For many years Gastec has conducted research into a cost-effective and properly modulating low NOx domestic natural gas burner that requires neither a fan nor cooling. (Pulles and Creemers, 1999) CFX-4 with the four-step scheme has been applied to analyse the design of this burner by Creemers (1999). In calculation like this, the coupled chemistry solver ensures fast and reliable convergence, despite the possible dominance of the reaction sources.

The model predicts the correct trends, especially the value and location of the maximum temperature, and also the correct portions of the flow split between the middle and side parts of the burner. Figure 20 shows the predicted temperatures from the central porous regions, and heat transfer to the heat exchanger. In the case shown here, the element thickness at the center has been halved to ensure flame stability under turn-down conditions. The results show that this causes partial blow-off of the flame at the center, whereas it remains flat close to the upper surface of the element at the sides. Complete combustion is predicted before the downstream boundary with a maximum flame temperature of about 1,850° C.

CONCLUSION

Coupled solvers are now being used extensively in CFD to improve the convergence of calculations, especially those with large numbers of cells and highly non-linear source terms involving multiple phases and/or many species. For these types of problem, their extra computational overhead compared to traditional segmented solvers is more than compensated for by their higher convergence rate and robustness.

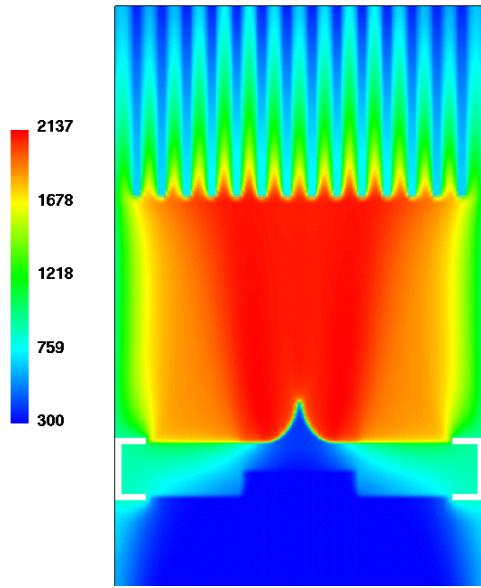


Figure 20: Predicted temperature (in Kelvin) for a Gastec domestic gas burner with a porous plug stabilizer and heat exchanger fins.

THREE-PHASE MIXING IN STIRRED TANKS

Mixing vessels are widely used in the chemical and process industries but their design and operation is often based on engineering experience and intuition rather than on detailed analysis. This situation is being changing rapidly by the introduction of CFD models of stirred tanks using the sliding grid approach.

Simon Lo (1999) of AEA Technology, in collaboration with the Mitsubishi Chemical Company, is validating the Eulerian-Eulerian multi-phase model in CFX-4 for a mixing vessel with three impellers as shown in Figure 21. In the sliding grid approach, a separate body-fitted mesh is constructed for the two domains: the rotating inner domain containing the impellers and shafts, and; the stationary outer domain with the vessel walls and baffles. The two domains are then matched on a cylinder with a radius chosen to lie between the impellers and the vessel walls. The total size of the model was 75,000 cells.

In the experiments of Dohi et al. (1999), a vessel of diameter 0.8m was fitted with two downward pumping 45° pitched-blade disk turbines and a curved blade impeller on a common shaft. Water and glass beads provided the liquid and solid phases and air was introduced through spargers to give a third phase. Measurements included the shaft power, the particle concentration by suction probe and the gas hold-up by observation of the liquid surface.

The liquid-particle and liquid-gas drag force interactions were modeled using standard drag law correlations, assuming an ellipsoidal bubble shape. A solid pressure force was introduced to prevent the particle packing fraction exceeding the theoretical maximum. Turbulent dispersion of the particulate phase and the particle-induced turbulence were also modeled.

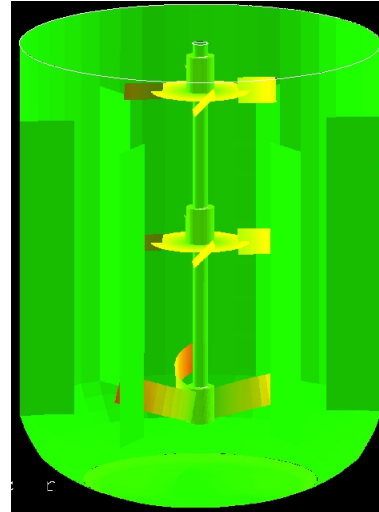


Figure 21: CFD model of a three-impeller mixing vessels using the sliding grid method to give exact representation of the vessel and impeller geometry.

Transient simulations were performed for several revolutions of the impeller shaft to ensure quasi-steady conditions. Typical time-averaged velocities and concentrations are shown in Figures 22, 23 and 24. A quantitative comparison between CFD and the experimental data of Dohi et al. is given in Table 6.

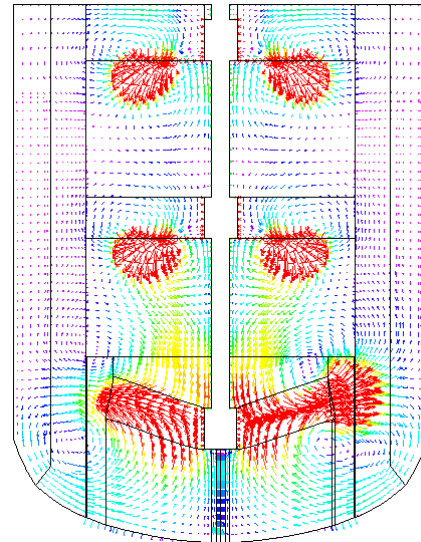


Figure 22: Liquid velocity predicted by the CFD model.

	Data (Dohi et al.)	CFD
Gas hold-up	0.12	0.12
Shaft power (W)	18	19
Solid concentration at lower probe (vol%)	28.3	30
Solid concentration at middle probe (vol%)	9	15
Solid concentration at lower probe (vol%)	4	1

Table 6: Comparison between CFD simulation and experiment for a three-impeller mixing vessel.

From these results, and others for a similar vessel of 0.2m diameter, it is concluded that the shaft power, gas hold-up and solid concentration can be predicted within $\pm 20\%$. The model seems to work equally well for any size of the vessel making it a useful tool for scaling-up analysis.

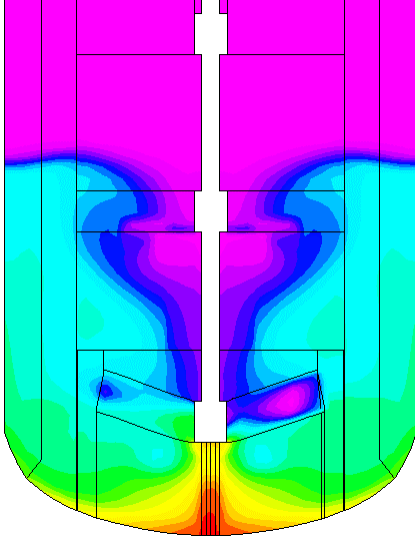


Figure 23: Particle concentration predicted by the CFD model.

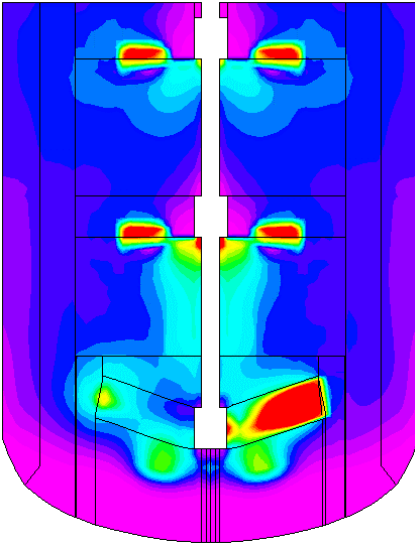


Figure 24: Bubble concentration predicted by the CFD model. Note the high concentration behind the blades.

SOLIDIFICATION MODELING

Many industrial processes, such as metal casting, welding and glass manufacture, are concerned with flows in the presence of melting and solidification. CFD simulation of flows involving phase changes is difficult because of the need to model the exchange of mass, momentum and energy between the different phases and to determine the location of the interface between the phases.

These problems were addressed by Bennon and Incropera (1987) who summed the full Navier-Stokes, continuity and energy equations for multi-phase flow over all phases to recover the usual single-phase equations for incompressible flow with additional momentum source term

$$c_{\alpha\beta}^{(d)} (\mathbf{U}_C - \mathbf{U}_L)$$

And the extra enthalpy source term

$$-\rho L \left(\frac{\partial f_L}{\partial t} + \mathbf{U}_C \cdot \nabla f_L \right)$$

where \mathbf{U}_C is the casting (or solid) velocity and the inter-phase drag coefficient, $c_{\alpha\beta}^{(d)}$, is given by the Carman-Kozeny equation

$$c_{\alpha\beta}^{(d)} = \mu_L C_D \frac{(1 - f_L)^2}{f_L^3}$$

where μ_L is the laminar viscosity of the liquid and C_D is the drag coefficient. Implicit in this formulation is the assumption that the solid and liquid phase densities are constant and equal and that both phases have the same local temperature.

The liquid fraction, f_L , varies non-linearly with temperature between the solidus and liquidus temperatures

$$f_L = \left(\frac{T - T_S}{T_L - T_S} \right)^m$$

Simple iterative procedures for updating f_L are known to destabilize convergence of steady-state calculations unless excessive under-relaxation or transient simulation are used. In CFX, the solidification model has been implemented using a development of Voller (1991) that allows steady-state calculations to be performed with a minimum of under-relaxation.

CONTINUOUS STEEL CASTING

In a collaboration between AEA Technology and Kvaerner Metals Continuous Casting, Hamill and Lucas (1999) have applied this model to the simulation of a thin-slab continuous casting mould and submerged entry nozzle. Liquid steel from the tundish flows continuously into the mould through the nozzle. The walls of the mould, which are made of copper, are water-cooled causing the outside of the steel to solidify. The steel is then withdrawn continuously from the mould.

By adding the source terms of Bennon and Incropera, the model can include the effects of the evolution of latent heat as the metal solidifies, and the forcing of the metal velocity to the casting speed in the solid shell. In the mushy region, where both solid and liquid phases are present, the Darcy-type resistance sources represent the flow of liquid through the solid crystal matrix. Sink terms in the turbulence equations are also applied to prevent turbulent transport in the solid shell.

The model prediction for typical operating conditions is presented in Figure 25. The vertical slices show the liquid fraction f_l , the mould walls are colored with temperature and the black lines are the flow streamlines in the melt. The steady build-up of the solid phase near the walls as the melt flows away from the nozzle is clearly visible as is the centerline recirculation in the jet from the nozzle.

During casting, argon is injected into the pouring tube to prevent the build up of deposits on the nozzle and to help clean the melt in the mould by encouraging the rise of solid inclusions to the free surface. By combining the solidification model with the two-phase bubbly flow model in CFX-4, the CFD model is able to predict the effect of argon injection (see Figure 26). Figure 27 shows the significant differences in the melt flow near the nozzle. The figure also shows the predicted gas concentration.

By applying the algebraic slip model, it is also possible to investigate the motion of inclusions within the melt as they rise to form a slag layer at the free surface, as shown in Figure 28.

In conclusion, the solidification model, combined with the bubbly-flow and algebraic slip models, offers the potential to investigate many important phenomena and to optimize particle removal rates by redesigning pouring tubes and submerged entry nozzles and positioning weirs and dams within tundishes.

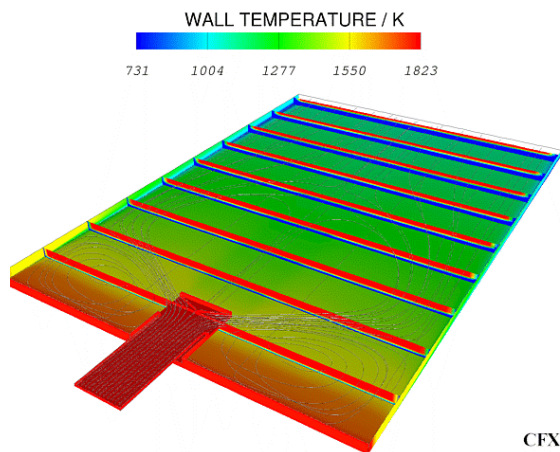


Figure 25: CFX prediction for continuous steel casting without argon injection.

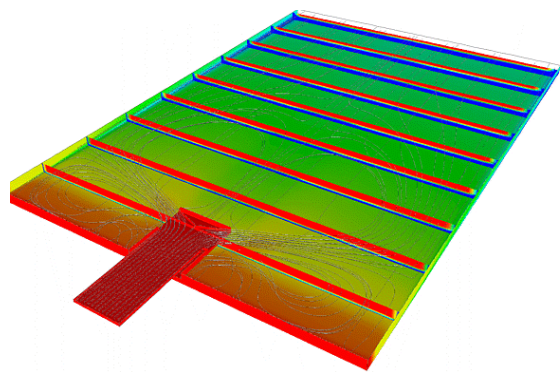


Figure 26: CFX prediction for continuous steel casting with argon injection.

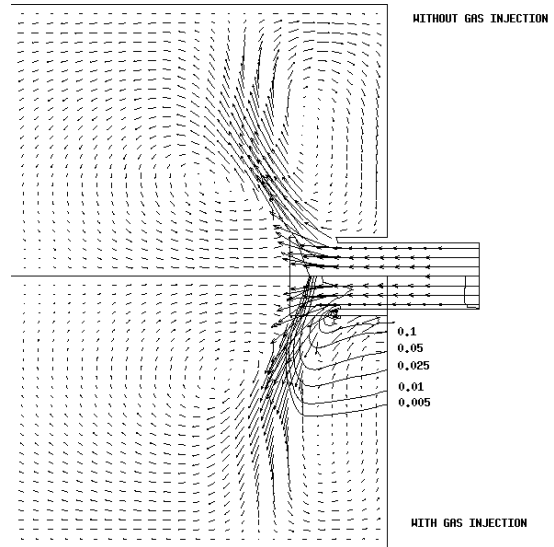


Figure 27: Mean velocities near continuous steel casting nozzle with and without argon injection. The contours show the argon volume fraction.

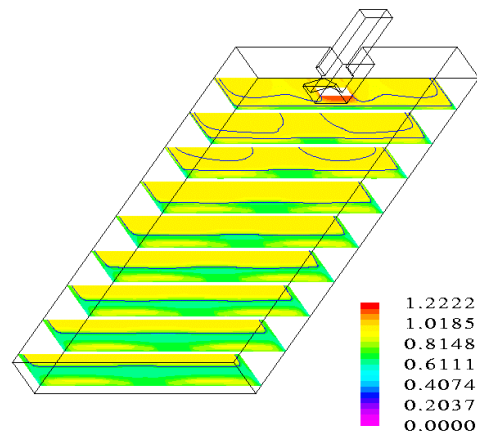


Figure 28: Solid inclusion concentrations as fraction of inlet concentration in continuous steel casting tundish.

INTEGRATED SOFTWARE SOLUTIONS

Due to the combined pressures of steadily-increasing model complexity and shortening project time scales, industrial engineers are finding it more and more difficult to master and apply the latest CFD technology to their problems. Furthermore, there is less time to communicate CFD results to their managers who have to make important investment decisions and risk evaluations.

As a result, there is a growing demand for customized and integrated software that will automatically read plant data, generate suitable meshes, run the model and deliver industry-standard outputs in the shortest possible time. Several packages of this type have been created recently incorporating CFX software for various applications, including combustion, mixing and continuous casting.

ACORDE Project

The furnace modeling for Sines Power Station (described earlier) forms part of a project to deliver an on-line software tool for power plant operators. The ACORDE software is built around a knowledge-based expert system (Azevedo et al., 1999) that is linked to the plant control monitoring system and advises the operator of non-optimal operation and recommends remedial action.

The software uses built-in physical models of flow and heat transfer (CFD and simpler zone models), boiler steam-side heat transfer and thermal efficiency, gaseous emissions (CFD and neural networks) and plant degradation (Neves et al., 1999). With these models it is possible for the operator to ask what-if questions, for example, "What would be the effect on NOx emissions of reducing the coal flow to the upper row of burners?" The furnace CFD models are too large to operate on-line and so the results are pre-calculated, stored and interpolated to the required boundary conditions.

ACORDE is being tested at Sines and also used for operator training by the Spanish utility, ENDESA S.A. In future, it is planned to extend the software to fluidized bed combustion, chemical plant and cement production.

Tokyo Gas Intelligent Support System

Tokyo Gas Energy Technology Research Institute has developed a furnace analysis environment called IF-DISS (Industrial Furnace Design Intelligent Support System). IF-DISS is a user-friendly interactive system customized for CFD analysis of industrial furnaces. It is being used extensively in the design of new types of gas-fired combustion equipment at Tokyo Gas, for example, muffle-type heat treating furnaces. In this type of plant, it is very important to heat the muffle in the center uniformly, something that Tokyo Gas succeeded in doing through the systematic investigation and optimization of the positions of their regenerative burners using CFX-4.

At present, IF-DISS Version 2 is being developed as a consortium project by Japan's three largest gas suppliers, Tokyo Gas, Osaka Gas and Toho Gas. The features of this latest version are:

1. A user-friendly interactive system which enables easier specification of geometry and operating conditions;
2. CFX command files and geometry files are to be output directly;
3. Mathematical models for burners and other heated elements and also physical properties of metal, fuel and combustion gas are stored in a database;
4. Convenient mesh generation tool is available;
5. Using the JAVA language, there will be INTRANET communication through an in-house PC network. In the future, INTERNET will be considered though it is not realistic now because of the high data transfer requirement.

CFX-ProMixus

CFX-ProMixus is a software package for modeling cylindrical mixing vessels using pre-assembled generic geometry and based on any CFX solver. A set of templates are used to include any standard impeller design and the vessel bottom can be flat, elliptical or conical. Up to five

constituent components are allowed, either Newtonian or non-Newtonian.

The software has been designed to run at three different levels, Express, Expert and Department, according to the level of experience of the users. "Department" level is aimed at those companies which have a group of expert users but want to propagate the use of CFD to process engineers without specialist knowledge of CFD. For portability, the user interface is written in JAVA with results printed in HTML (web) format.

Continuous Casting

For a large metals processing company, AEA Technology has developed integrated software that enables process engineers to request CFD-TASCflow calculations in a batch mode and return results in a standard format. As for IF-DISS, all communication between engineers and CFD specialists is handled by an Intranet system. Although the software will process calculations automatically, it allows the CFD specialists to intervene to change priorities or modify the calculations if appropriate. Figure 29 is the main menu of the GUI-based input tool and shows the mimic of the system which is used to input the main variables into the model.

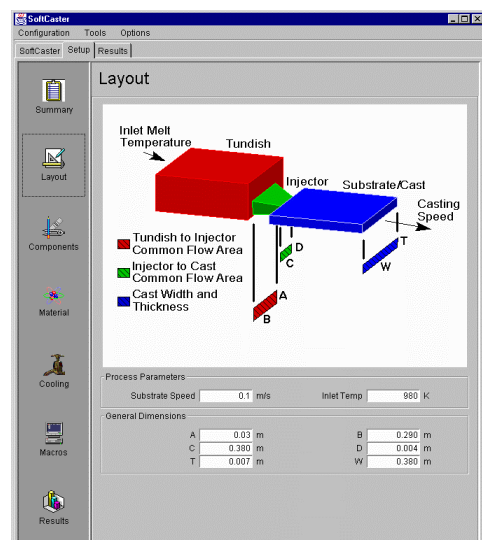


Figure 29: Graphical User Interface for an integrated software tool to process continuous casting calculations using CFX-TASCflow.

OVERALL CONCLUSIONS

Even with existing physical models, CFD can offer cost-effective solutions for many complex systems of interest to the power generation, process and metals industries. Examples have been presented for coal-fired furnaces, laminar combustion, mixing vessels and continuous metal casting but these are typical of many CFD models involving complex multi-phase flows and reacting systems that are currently being modeled.

Thanks to improved ease-of-use and, in particular, the development of customized software built around CFD models, the use of CFD is no longer a specialist activity but is accessible to process engineers, plant operators and managers. Integrated software can also accelerate the pace of development and improve the communication of results throughout a large organization.

ACKNOWLEDGEMENT

The author gratefully acknowledges the help of his colleagues, Ian Hamill, Ian Jones, Richard Lonsdale, Simon Lo and Mark Turrell. We would also like to acknowledge the support and cooperation of Burns & McDonnell, Gastec, International Combustion, Kvaerner Metals, Mitsubishi Chemical Company, Southern Company, Tokyo Gas, the UK Department of Trade and Industry and the European Commission.

REFERENCES

AEA TECHNOLOGY (1997), "CFX-4.2: solver manual", *CFX International*.

AZEVEDO, J. et al. (1999), "On the development of a knowledge base and an expert system shell language for emissions minimization and boiler optimization", *Presented at 5th Int. Conf. "Technologies and combustion for a clean environment", Lisbon, 12-15 July 1999*.

BENNON, W.D. and INCROPREA, F.P., (1987), "A continuum model for momentum, heat and species transport in binary solid-liquid phase change systems - I. Model formulation", *Int. J. Heat Mass Transfer.*, **30**, 10, pp. 2161-2170.

CHEN, W., SMOOT, L.D., HILL, S.C. and FLETCHER, T.H., (1996), "Global rate expression for nitric oxide reburning", *Energy & Fuels*, **10**, pp.1046-1052.

CREEMERS, B.W., (1999), "Modellering honingraat-brander, Deelstudie van het onderzoek Stabiliteit van Laminaire Vlammen", *Gastec report HGT/640/CS*.

DOHI, N., MATSUDA, Y., ITANO, N., MINEKAWA, K. and KAWASE Y., (1999), "Solids suspension in multi-impeller three-phase stirred tank", *3rd Int. Symposium on Mixing in Industrial Processes*, 19-22 September, 1999, Osaka, Japan.

HAMILL, I. and LUCAS, T., (1999), "Computational fluid dynamics modeling of tundishes and continuous casting moulds", *Proc. Symp. Fluid Flow Phenomena in Metals Processing*, 28 February-4 March, 1999, San Diego, CA, ed. N. El-Kaddah et al., pp. 279-286.

JONES, W.P. and LINDSTEDT, R.P., (1988), "Global reaction schemes for hydrocarbon combustion", *Combust. Flame*, **73**, 233-249.

LO, S., (1999), "Modeling of multi-phase flows in multi-impeller stirred vessels", *Hydrotransport 14 Conf.*, 8-10 September, 1999, Maastricht, The Netherlands.

MALLENS, R., (1996), "Stabilization of laminar premixed methane/air flames", Doctoral thesis, Technical University of Eindhoven, The Netherlands, December 1996.

NEVES, M., GIMENEZ, A. and CARVALHO, M.G., (1999), "Development of advanced control methodologies using reliable multi-detection sensors for boilers", *Power Gen. Europe Conf., Germany*.

O'CONNOR, M., (1999), "The effects of coal quality on NO_x emissions and carbon burnout in pulverized coal-fired utility boilers", *UK Dept. Trade and Industry Report No. COAL R153*.

PULLES, K. and CREEMERS, B.W., (1999), "Niks uitontwikkeld, Tijdschrift in de Energiemarkt", *GAS, May 1999*.

VOLLER, V.R. and SWAMINATHAN, C.R., (1991), "General source-based method for solidification phase change", *Numer. Heat Transfer B*, **19**, pp.175-189.